Check for updates

ARTICLE　OPEN

North Atlantic subpolar gyre provides downstream ocean predictability

Hongdou Fan [1,2 ✉], Leonard F. Borchert [1], Sebastian Brune[1], Vimal Koul [1,3] and Johanna Baehr[1]

Slowly varying large-scale ocean circulation can provide climate predictability on decadal time scales. It has been hypothesized that the North Atlantic subpolar gyre (SPG) exerts substantial influence on climate predictability. However, a clear identification of the downstream impact of SPG variations is still lacking. Using the MPI-ESM-LR1.2 decadal prediction system, we show that along the Atlantic water pathway, a dynamical link to the SPG causes salinity to be considerably better predicted than temperature. By modulating the slow northward ocean propagation, the subsurface memory of SPG variations enables salinity to be skillfully predicted up to 8 years ahead. In contrast, the SPG loses influence on temperature before Atlantic water penetrates into the Nordic Seas, and in turn, limits temperature to be predicted only 2 years ahead. This study identifies the key role of SPG signals in downstream prediction and highlights how SPG signals determine prediction time scales for different quantities, opening the door for investigating potentially associated predictions in the subarctic for the earth system, marine ecosystems in particular.

INTRODUCTION

The poleward propagation of thermohaline anomalies in the North Atlantic Ocean provides oceanic and continental climate predictability on decadal time scale[1–3]. However, previous studies have not identified whether the variations of the Subpolar Gyre of the North Atlantic (SPG) exert influence on the downstream ocean prediction[4]. In this study, we investigate the role of the SPG in decadal prediction along the Atlantic water pathway with emphasis on subsurface temperature and salinity, demonstrating a robust connection for the latter.

It has been documented that the high predictability of the SPG resides in the initialization and persistence of the Atlantic meridional overturning circulation (AMOC), and ocean dynamics over the subpolar North Atlantic[5,6]. Understanding the downstream impact of the SPG is crucial for earth system prediction in the subarctic[2]. Several studies showed that the SPG dominates properties of the Atlantic Inflow into the Nordic Seas by modulating the proportion of subpolar and subtropical waters in the Atlantic Inflow on interannual to decadal time scales[7–10]. A strong SPG feeds cold and fresh subpolar water to the Atlantic Inflow, while a weak SPG allows the northward extension of warm and saline subtropical water. Downstream of the SPG, via the North Atlantic Current, the Norwegian Atlantic Current advects across the Faroe-Iceland Ridge and the Faroe-Shetland Channel and circulates in a counterclockwise direction in the Nordic Seas[11,12]. It takes 3–7 years for the upper ocean anomalies to progress from the eastern SPG to the Fram Strait and Barents Sea[13,14]. The well-identified high predictability of the SPG[5,6] together with its prominent influence on the slow northward propagation of thermohaline anomalies hints at potentially high decadal predictability in the downstream ocean.

Efforts have been taken to explore the impact of the SPG on the predictability of downstream sea surface temperature (SST) in dynamical prediction systems[4], but the manifestation of SPG signals in the downstream upper ocean prediction has not been clearly identified. Significant SST skill along the Atlantic water pathway is limited to 1–2 lead years in dynamical prediction systems[2], rather than a decade as demonstrated in an observation-based study[15]. Research from a forced ocean model indicated that SST along the Atlantic water pathway is more dominated by the overlaying atmospheric interannual variability than subsurface variability[16], implying that the impact of the SPG may manifest in the prediction of subsurface ocean. Recent studies revealed a close linkage between the SPG and the subsurface salinity in the Barents Sea[14], and showed that the SPG signals can lead to skillful statistical prediction of fish stocks in the Barents Sea a decade in advance[6]. The evident impact of the SPG on the downstream salinity prediction, but unclear impact on the SST prediction, agrees well with notions that salinity anomalies along the Atlantic water pathway mostly remain unchanged, while temperature anomalies are modified by the atmosphere through surface heat fluxes[6,17,18].

To disentangle the connection of SPG variations with temperature and salinity prediction along the Atlantic water pathway, we carry out a comparison of prediction between salinity and temperature along the Atlantic water pathway with emphasis on forecast lead years 3–5, for the period 1970–2019. Then, we examine the propagation of SPG signals based on lag correlation and composite results, and investigate the impact of SPG signals on prediction skill at individual forecast lead years. Here, the retrospective initialized decadal predictions (hindcasts) are based on the Max-Planck-Institute Earth System Model version 1.2, low-resolution set up (MPI-ESM-LR1.2). The corresponding assimilation experiment (ASSIM) is employed as observational reference. We use anomaly correlation coefficient (ACC) metrics to evaluate the agreement between hindcasts and ASSIM (see Methods).

[1]Center for Earth System Research and Sustainability, Universität Hamburg, Hamburg, Germany. [2]International Max Planck Research School on Earth System Modelling, Max Planck Institute for Meteorology, Hamburg, Germany. [3]Now at the Cooperative Institute for Modeling the Earth System, Princeton University, Princeton, NJ, USA. ✉email: hongdou.fan@uni-hamburg.de
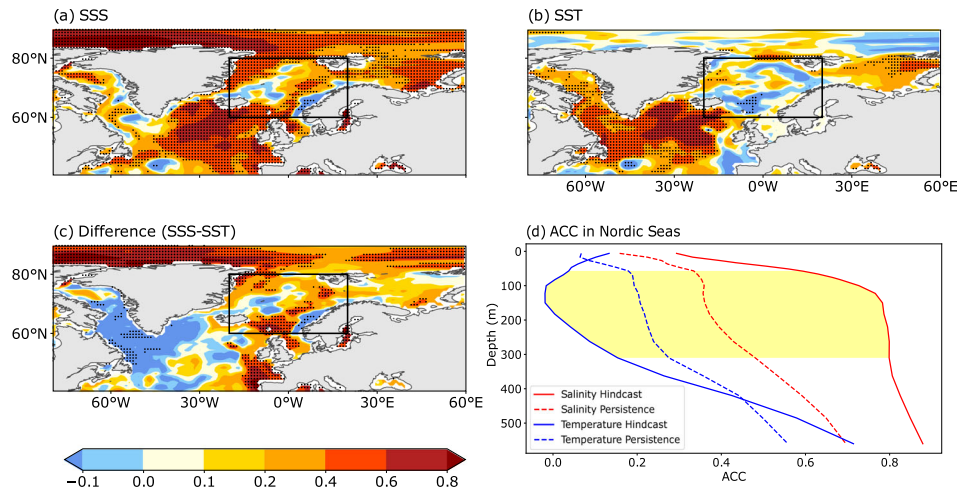
Fig. 1 The anomaly correlation coefficient (ACC) and ACC difference for detrended annual mean salinity and temperature at lead years 3–5. ACC between hindcast and ASSIM for (**a**) sea surface salinity (SSS), **b** sea surface temperature (SST) for the period 1970–2019. **c** ACC difference between SSS and SST in hindcast. **d** ACC in hindcast (solid line) and persistence (dash line) for salinity (red) and temperature (blue) at different depths in the Nordic Seas for the period 1975–2019. Stippling in (a)-(c) denotes the ACC or ACC difference is significant at 95% confidence level based on block bootstrapping. Yellow shading in (**d**) denotes the ACC difference between salinity and temperature in hindcast is significant at 95% confidence level based on block bootstrapping. The box outlined in black in (**a**)–(**c**) shows the area used to calculate the ACC in the Nordic Seas.

RESULTS

Salinity is better predicted than temperature along the Atlantic water pathway

We first assess the prediction skill of sea surface salinity (SSS) and sea surface temperature (SST) at lead years 3–5 in the northern North Atlantic (Fig. 1a, b). The SSS is skillfully predicted in the eastern SPG region. SST is slightly better predicted than SSS, which agrees with Borchert et al.[5] that models generally show high SST skill in the SPG region. However, the skill of SSS is higher than the skill of SST along the Atlantic water pathway, especially in the Nordic Seas (Fig. 1a, b). This difference in skill (Fig. 1c) is significant over the eastern and western Nordic Seas, where the Atlantic water anomalies move northward and southward, respectively. The ACC difference between salinity and temperature along the Atlantic water pathway is robust with EN4[19] and Atlas[20] as observational references (Supplementary Fig. 1).

To further understand the ACC difference between salinity and temperature along the Atlantic water pathway, we choose the Nordic Seas (box in Fig. 1a) as representative and compare the ACC from hindcasts with ACC from persistence at different depth layers in the Nordic Seas (Fig. 1d). Here, we use a statistical persistence forecast as a reference when evaluating hindcasts prediction skill arising from model dynamics (see Methods). The ACC in both hindcasts and persistence generally increases with depth (Fig. 1d). This is expected because of the decreasing influence from the atmosphere. One notable exception is that ACC of temperature in hindcasts first decreases with depth until about 100 m, and then increases. Dynamical predictions for salinity and temperature perform sharply differently: the ACC of salinity, especially in the subsurface, is significantly higher than that of temperature, and this is also the case for their counterparts in persistence forecast. Moreover, the ACC of salinity from hindcasts is higher than the ACC from persistence in all depth layers above 500 meters (Fig. 1d). In contrast, the ACC of subsurface temperature from hindcasts is even lower than ACC from persistence. Salinity and temperature both show general high ACC in the SPG region (Fig. 1a, b), but they have discrepancy along the Atlantic water pathway. We conjecture from these findings that the SPG may play a stronger role in salinity prediction than that in temperature prediction along the Atlantic water pathway. To investigate a possible dynamical mechanism, we use a density-based SPG index (Fig. 2a; see Methods), which captures the connection between SPG variability and water properties in the eastern subpolar North Atlantic[21], and we use the depth-averaged anomalies over 150–310 meter as representative of subsurface properties in the remaining part of this study.

Poleward propagation of SPG signal and its impact on prediction skill

We investigate the co-variability of the SPG variations and salinity and temperature changes in the northern North Atlantic using lagged correlation analysis. Subsurface salinity in the Nordic and Barents Seas is significantly correlated with SPG variability (Fig. 2b). The prominent salinity anomalies induced by the SPG propagate into the Nordic Seas after 3–5 years. In comparison, downstream temperature is less correlated with SPG variability (Fig. 2c), and the lag correlation is only significant in the northwestern Nordic Seas and western Barents Sea (Fig. 2c).

To study the influence of the SPG on salinity and temperature along the Atlantic water pathway, we define strong and weak SPG phases with above and below 0.5 standard deviation, respectively. Composite results (Fig. 3a–e) from hindcasts constructed from the difference between weak SPG phases and strong SPG phases further support the pronounced SPG influence on salinity along the Atlantic water pathway, especially in the Nordic Seas. After a weak SPG phase, positive salinity anomalies develop and persist in the SPG region and saline subtropical water dominates the Atlantic Inflow, penetrating into the Nordic and Barents Seas in the following 4 years. The saline water in the eastern SPG region flows across the Faroe-Iceland Ridge and the Faroe-Shetland Channel after 1 year (Fig. 3b), and moves along with the Norwegian Atlantic Current (Fig. 3c) into the Nordic Seas. The salinity anomalies arrive at the Fram Strait and Barents Sea after 3 years (Fig. 3d), reaching the western Nordic Seas along with the East Greenland Current (Fig. 3e).

Similar to positive salinity anomalies, positive temperature anomalies caused by a weak SPG persist in the SPG region and progress northward into the Nordic Seas. However, the regions in the Nordic Seas that show significant temperature anomalies are smaller, and temperature anomalies persist for a shorter period, when comparing counterparts from salinity anomalies (compare Fig. 3a–e, f–j). Positive temperature anomalies are only significant
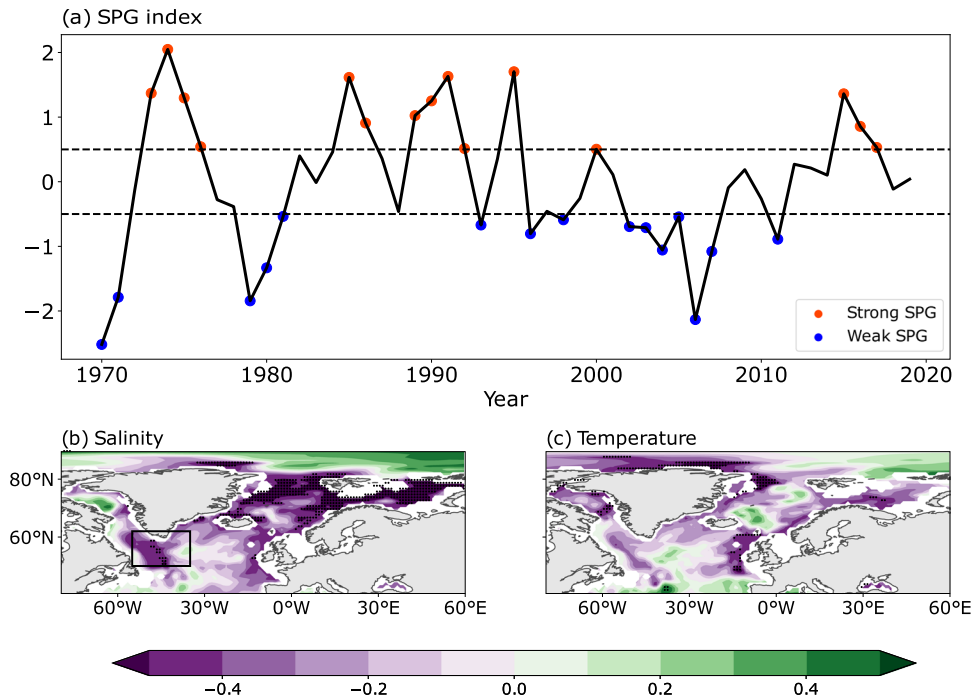
Fig. 2 Time series of the SPG index and its lag correlation with subsurface salinity and temperature anomalies for the period 1970–2019.
a Standardized time series of SPG index. Lag correlation between the SPG index and subsurface, **b** salinity and **c** temperature at lag years 3–5 (salinity and temperature lag SPG index) in ASSIM. The SPG index is defined as density anomaly at 310 m depth over 55–35°W, 50–62°N [area outlined in black in (**b**)]. The positive (negative) SPG index indicates strong (weak) SPG circulation and strong (red dots) and weak SPG (blue dots) phases are identified with above 0.5 and below −0.5, respectively. Stippling in (**b**) and (**c**) denotes 95% confidence level based on Student's *t* test.

in the eastern Nordic Seas for 1–3 years (Fig. 3i, j) and are significant in the Barents Sea after 3 years (Fig. 3i, j). After 4 years, there are significant saline anomalies while less prominent warm anomalies in the Nordic Seas (Fig. 2e, j). For a strong SPG phase, similar results appear for the propagation of less saline and cold anomalies, respectively. The results suggest that the SPG exerts a weak influence on temperature along the Atlantic water pathway, while poleward ocean currents may play a role in connecting salinity in the Nordic Seas with the SPG strength.

We investigate the role of poleward propagation of salinity and temperature signals by following their propagation along the North Atlantic Current, 9 boxes (Fig. 4a) with size of 5° × 5° are selected along the North Atlantic Current-Norwegian Atlantic Current pathway, and centers of the boxes are consistent with Årthun et al.[15]. Hovmöller diagrams (Fig. 4b, d) show a clear tilt of anomalies in ASSIM, especially for salinity. When there are strong anomalies in the SPG (box 3 in Fig. 4a), salinity and temperature anomalies progress from the SPG to the Fram Strait (box 9 in Fig. 4a). For instance, induced by a weak SPG phase in 1970 and a strong SPG phase in 1990, both salinity and temperature anomalies propagate into the Nordic Seas after around 3–7 years, but less prominent for temperature. For a strong SPG phase in 1974 and a weak SPG phase in 1980, temperature anomalies show no clear propagation of signal into the Nordic Seas and are relatively constrained to the subpolar region or southern Nordic Seas (Fig. 4d). In contrast, salinity anomalies propagate all the way through to the Fram Strait and persist for several years (Fig. 4b). The propagation of the subsurface salinity and temperature signals is similar with the propagation of the SST signals found in a previous study[15]. Notice that low-pass filtering and a complex principal component analysis make the leading mode of SST propagation smooth (Fig. 5a in Årthun et al.[15]), still there are slight discontinuities at the Greenland-Scotland Ridge (compare Fig. 5a in Årthun et al.[15] and Fig. 4b–e). Inspection of the Hovmöller

diagrams from EN4 data indicates consistent results (compare Figs. 4b, d and 4c, e), suggesting that the salinity and temperature signals may be carried by poleward ocean currents modulated by the SPG variations.

To further understand the mechanism driving the poleward transport of signals, we decompose salt and heat transport anomalies at the Faroe-Shetland Channel into changes due to velocity anomalies, changes due to salinity or temperature anomalies, and changes due to eddy activity (Supplementary Fig. 2). Both the salt and heat transport anomalies are dominated by the velocity component, confirming the key role of ocean advection in volume transport anomalies[2,22]. However, the impacts of the salinity component and the temperature component terms, respectively, on the total transport anomalies are different. The amplitude of the salinity component is as small as that of the eddy component, and both are negligibly small compared to total transport anomalies. While the contribution of temperature component to total transport anomalies is comparable with that of velocity component in some years, even with negative contribution. These results indicate that ocean dynamics almost completely govern salt transport anomalies, and dominate heat transport anomalies. Temperature variability plays a subdominant role in heat transport anomalies, which explains why the link of the SPG to downstream salinity is stronger than that to downstream temperature. Downstream temperature exhibits pronounced interannual variability and has low signal-to-noise ratio. In addition, temperature anomalies tend to be modified by the negative feedback of air-sea flux[23], therefore the SPG signals are damped more in temperature than in salinity.

A lead-lag correlation analysis between the salinity anomalies along the Atlantic water pathway (boxes in Fig. 4a) and the SPG index further supports the different downstream influence of the SPG. The significant negative correlation stays in the subpolar North Atlantic when salinity leads the SPG index (Fig. 5a),
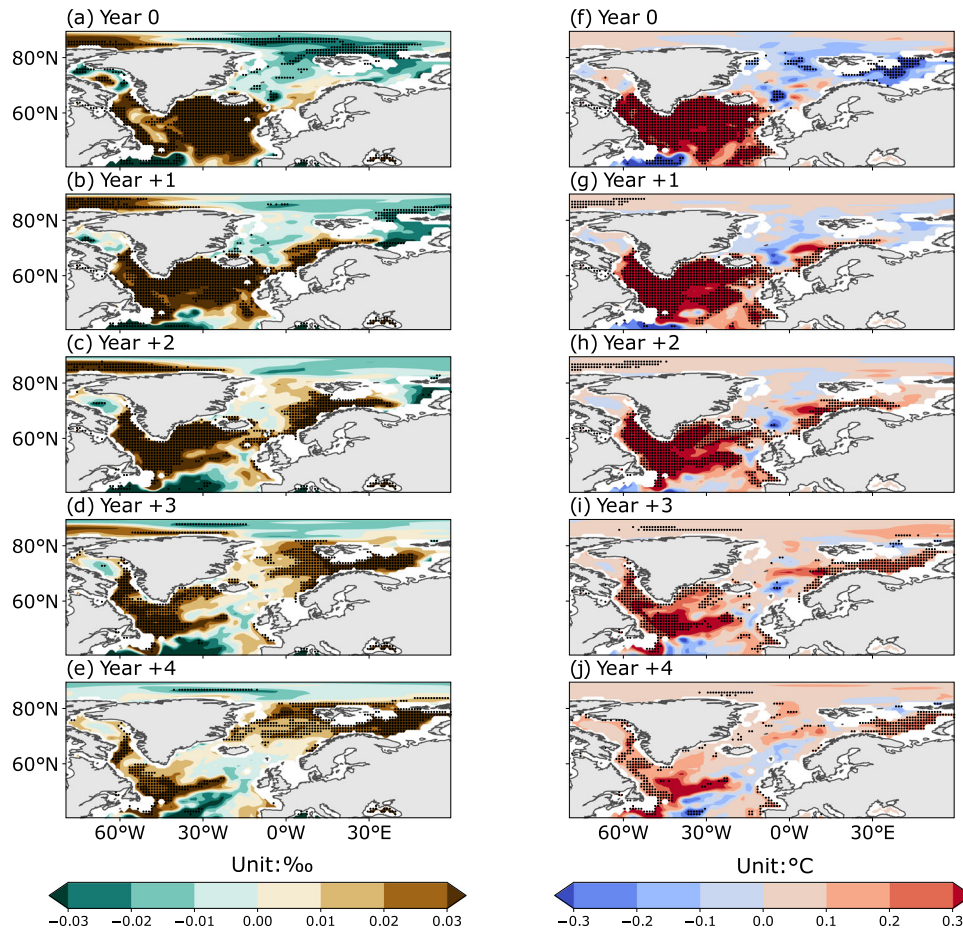
Fig. 3   Composite anomalies according to the SPG phases (weak phase minus strong phase). a–e Composite salinity anomalies from year 0 to year 4 according to the SPG phases in hindcast. **f–j** As in (**a**)–(**e**), but for temperature. Stippling denotes 95% confidence level based on bootstrap test. Strong and weak SPG phases are identified with above 0.5 and below −0.5 standard deviation of the SPG index, respectively.

indicating the origin of the signal is the subpolar North Atlantic rather than further south in the subtropics. The salinity signal propagates from the subpolar region (box 3 in Fig. 4a) to the Nordic Seas with increasing time lag in ASSIM. The salinity at the Fram Strait (box 9 in Fig. 4a) is significantly correlated with the SPG index from lag year 2 to lag year 6, indicating the persistent downstream influence of the SPG. The hindcasts reproduce the progression of the SPG signal to the Nordic Seas (Fig. 5b), with a slight discontinuity where the anomalies pass across the Faroe-Iceland Ridge and the Faroe-Shetland Channel (between box 5 and box 6 in Fig. 4a). This discontinuity is consistent with previous studies[6,16]. As a result, the prominent correlation between salinity and the SPG is persistent in different hindcast lead years, therefore we conclude that the model skillfully predicts the propagation of salinity signals from the SPG into the Nordic Seas. Benefiting from the poleward propagation and persistence of SPG signals, after lead year 3, the salinity in the eastern Nordic Seas is better predicted (Fig. 5c) than upstream for the same forecast lead year. The salinity in the northernmost Nordic Seas (box 9 in Fig. 4a) is skillfully predicted at lead year 8 when the ACC in subpolar regions becomes negative.

Temperature shows a similar pattern for cross-correlation as salinity (compare Fig. 5a and d). When temperature leads the SPG index, the significant correlation stays in the subpolar North Atlantic. When the SPG index leads temperature, the correlation is less prominent comparing to salinity. There is no clear poleward propagation of the temperature signal in ASSIM, which is also the case for the hindcasts (Fig. 5e). This may be

due to that temperature signals are damped due to negative feedback of air-sea flux[23] along the Atlantic water pathway. Consequently, the ACC of temperature along the ocean currents is generally lower than ACC of salinity (compare Fig. 5c and f), except in the eastern subpolar North Atlantic (box 4 in Fig. 4a). The shallow Greenland-Scotland ridge (box 6 in Fig. 4a) has a large negative influence on temperature prediction, where temperature ACC drops to zero after lead year 1. The ACC of temperature in the Nordic Seas becomes negative after 2 or 3 lead years. Unlike salinity, the influence of the SPG on temperature prediction skill is constrained to the subpolar region. The different influence from the SPG manifests itself, especially after lead year 4, when high ACC of salinity moves northward to the Nordic Seas while ACC of temperature becomes negative and shows no further poleward propagation. The findings are robust when we use a SPG index based on sea surface height (SSH) anomalies for cross-correlation with salinity and temperature, and when we use EN4 as reference to evaluate the ACC along the North Atlantic pathway (Supplementary Figs. 3 and 4). As discussed earlier, temperature variability also plays a role in heat transport anomalies and is largely influenced by the atmospheric variability[16]. This difference between salinity and temperature lead to the stronger link of the SPG to downstream salinity than that to downstream temperature. These results further manifest that downstream salinity is better predicted than temperature due to this stronger dynamical links to the SPG.
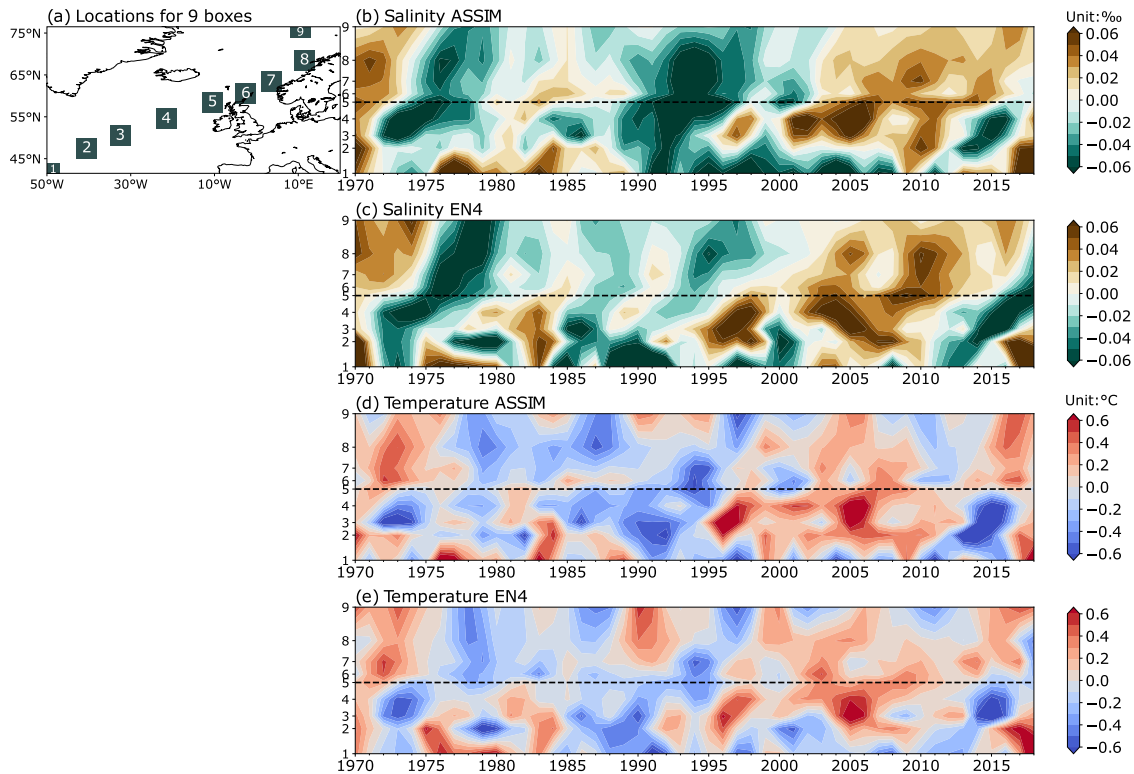
Fig. 4 Poleward propagation of subsurface salinity and temperature anomalies along the Atlantic water pathway. a 9 green boxes as representative along the Atlantic water pathway[15]. Hovmöller diagrams of subsurface salinity anomalies along the Atlantic water pathway from (**b**) ASSIM and (**c**) EN4. **d**, **e** As in (**b**), (**c**), but for temperature. The dashed line in (**b**)–(**e**) approximates the Greenland-Scotland Ridge. Time series for 9 boxes are 3–30-yr band-pass filtered for illustrative purposes.
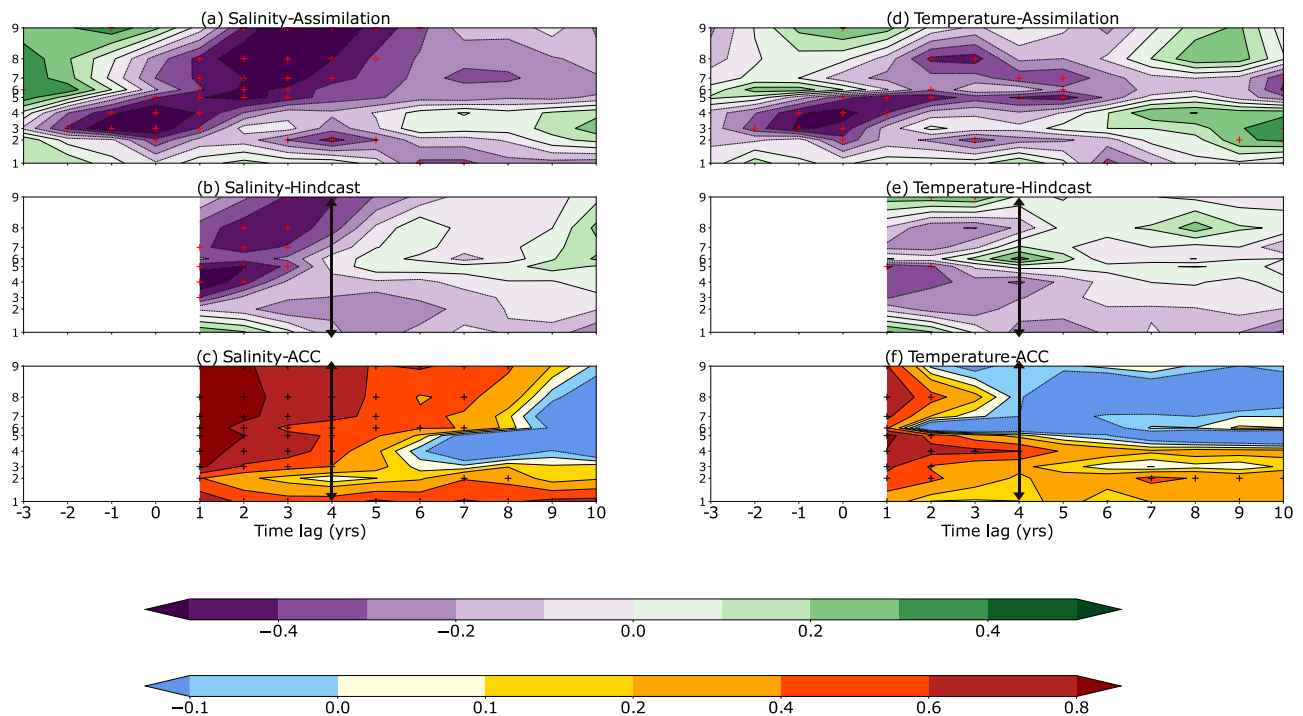
Fig. 5 Cross-correlation coefficients and ACC along the Atlantic water pathway. Cross-correlation between the SPG index and subsurface salinity along the Atlantic water pathway (green boxes in Fig. 3a) from (**a**) ASSIM and (**b**) hindcast. The x-axis in (**b**) denotes the lag years for cross-correlation (salinity lags the SPG) and the hindcast lead years for salinity. **c** ACC for salinity at different hindcast lead years. **d**–**f** As in (**a**)–(**c**), but for temperature. Stippling in (**a**), (**b**), (**d**) and (**e**) denotes 90% confidence level based on Student's t test. Stippling in (**c**) and (**f**) denotes 95% confidence level based on block bootstrapping. The black arrows in (**b**), (**c**), (**e**), (**f**) highlight the lag (lead) years 4.

DISCUSSION

Based on the MPI-ESM-LR1.2 decadal prediction system, we show that the SPG contributes to the high performance of downstream salinity prediction by modulating salt transport anomalies. Our results support that the poleward propagation of thermohaline anomalies is essential for subarctic decadal prediction[2,15,16], and the hindcasts capture this physical process for salinity along the Atlantic water pathway properly. We confirm that the SPG plays a key role in modulating water properties in the Atlantic Inflow into the Nordic Seas[6,7]. We further demonstrate that SPG signals contribute to salinity prediction, which in turn may benefit earth system prediction in the subarctic, including fishery predictions as well as predictions of habitat of vulnerable species[24]. In contrast to salinity, models show low predictive skill for temperature along the Atlantic water pathway[2,4] and temperature anomalies propagate downstream only to a limited degree[2]. In general, decadal prediction systems and their underlying models may differently represent the ocean dynamics behind the propagation of salinity and temperature signals and the air-sea interaction, either due to model bias or due to the initialization procedure. One can expect some impact on the prediction skill. Nevertheless, in terms of the prediction skill of SST in the SPG, for example, MPI-ESM is not significantly different from other models[25].

It is interesting to notice the different link of the SPG to downstream salinity and temperature, and the discrepancy of their predictive skill. Velocity anomalies of ocean currents drive both salt and heat transport anomalies as previous studies concluded[2,22]. Nevertheless, downstream temperature shows pronounced interannual variability and has low signal-to-noise ratio, and temperature anomalies are more impacted by air-sea interaction[11,23] than salinity anomalies. This may explain why the dynamical link of the SPG to downstream salinity is stronger than that to downstream temperature. Consequently, the SPG signals benefit salinity but not temperature prediction. Further investigation into the low-temperature prediction skill along the Atlantic water pathway[2,4] is beyond the scope of this study. Given that the prediction skill of temperature in the Nordic Seas is even lower than persistence, we speculate that MPI-ESM-LR1.2 may have model issues that may degrade temperature prediction, for example, ocean models may have difficulties in simulating mesoscale activity at narrow channels[2], which would impact the signal transition through the Faroe-Shetland Channel. How the representation of air-sea interaction[11,23] in models plays a role in low predictability of temperature is also worth further investigation.

On the other hand, temperature anomalies do propagate from the SPG to the downstream in some years. The difference between salinity and temperature anomaly propagation is that temperature signals tend to break at the Greenland-Scotland ridge. We notice that both salinity and temperature anomalies have some disconnects (dashed line in Fig. 4b–e) around Faroe Ridge and the Faroe-Shetland Channel. This discontinuity of anomaly propagation for both salinity and temperature indicates that the shallow Greenland-Scotland Ridge is a challenge for prediction due to the complex shelf-sea dynamics[6]. The poor correlation of temperature between south of the Greenland-Scotland Ridge and downstream is common for ocean models[2], and also can be seen in EN4 in our study. To the north of the Greenland-Scotland Ridge, temperature shows high lead-lag correlation with temperature at the Fram Strait, anomalies propagating from Faroe-Iceland Ridge to the Fram Strait in ASSIM (Supplementary Fig. 5a, c). Similar results (Supplementary Fig. 5b, d) from the historical runs support that MPI-ESM-LR is capable of simulating mechanism of anomaly propagation. Besides, different observational datasets show uncertainty at the Greenland-Scotland ridge[1]. Fully addressing the discontinuity of anomaly propagation with currently available observational data is hardly possible.

We conclude that the SPG provides downstream ocean predictability by modulating volume transport anomalies along the Atlantic water pathway. We further highlight that the SPG signal can manifest itself differently in downstream salinity and temperature, which leads to different prediction skill for temperature and salinity in the same model. The link of the SPG to downstream salinity is stronger than that to downstream temperature, and therefore salinity is better predicted than temperature. The significant SPG-induced temperature anomalies persist up to the eastern Nordic Seas for 2–3 years, and are skillfully predicted up to 2 years ahead. In contrast, SPG-induced salinity anomalies persist into the Nordic Seas significantly for 6 years, and are skillfully predicted up to 8 years ahead. Our results reveal that the manifestation and persistence of SPG signals determine the prediction time scales of downstream ocean climate. This study firmly establishes the prominent role of ocean circulation in downstream ocean predictability, illuminating the imprint of ocean dynamics in the subarctic climate prediction and opening the door for investigating potentially associated downstream predictability for the earth system, marine ecosystems in particular.

METHODS

Decadal prediction system

In this study, we use retrospective forecasts (Hindcasts) from our decadal prediction system based on MPI-ESM-LR1.2[26,27]. The 16-member hindcast ensemble is initialized from a 16-member weakly coupled assimilation experiment (ASSIM) each November 1st from 1960–2019[28–30] and run for 10 years. We thus analyze the hindcasts for their common time frame 1970–2019. The assimilation covers the time period 1958–2020 and consists of a 16-member oceanic Ensemble Kalman filter[31] that assimilates monthly temperature and salinity profiles from EN4[19] using the Parallel Data Assimilation Framework[32] (PDAF). There is no assimilation of satellite derived SST. The availability of in-situ observations of North Atlantic temperature is slightly better than that of salinity, therefore the nominal observational coverage of temperature over the whole time period 1958–2020 is larger than that of salinity. However, in practical terms of monthly averaged profiles available to the assimilation, there is no big difference between temperature and salinity, with the largest differences in the 1960s, and almost no difference with the Argo floats[33] in place from 2004 onward. In each assimilation member, atmospheric temperature, vorticity, and divergence at all atmospheric levels above 900 hPa, as well as surface pressure are nudged to ERA40/ERA-Interim/ERA5 reanalysis[34–36]. There is no direct assimilation of atmospheric surface temperature. Both assimilation and hindcasts use external forcing according to CMIP6[37], with historical forcing until 2014 and SSP245 assumed after 2014. More details on the decadal prediction system can be found in Polkova et al.[30] and Brune and Baehr[28].

Observational references

We utilize ASSIM and two other observation-based datasets, EN4 analysis[19], and Atlas[20] as observational reference to investigate the skill of decadal prediction. Please note that all three references are not independent, because Atlas profiles are contained in EN4 profiles, and ASSIM is ingesting EN4 profiles. However, results from EN4 analysis and Atlas are consistent with results from ASSIM (Supplementary Figs. 1 and 4). Atlas data doesn't cover the period of 2013–2019, which we would like to include in our analysis. Both ASSIM and EN4 analysis ingest the same sub-surface temperature and salinity profiles (from EN4), with different algorithms. Therefore, we decided to present our findings with the dynamically

consistent ASSIM rather than the statistically interpolating EN4 analysis as a reference in this paper.

Data processing

All hindcasts and ASSIM are linearly detrended and remapped to $1° \times 1°$ horizontal resolution prior to analysis. Monthly model output is averaged into yearly means, and yearly anomalies are formed against its climatology, which is defined as the 50-yr (1970–2019) mean of 16-member ensemble mean in hindcasts and ASSIM. No data filtering is applied in our study, except for Hovmöller diagrams where time series are 3–30-yr band-pass filtered for illustrative purposes. The persistence forecast is predicting future condition statistically based on past data, which is commonly used as a reference when evaluating dynamical prediction skill. In this study, the persistence forecast is constructed from ASSIM with the first order autoregression model. For fair comparison with hindcasts at lead years 3–5, we use a 3-yr average and predict next 3–5 years in autoregression model. The weight in space is considered when we calculate the area average[38]. In this study, we use water salinity at 6 m depth as SSS, and the depth-averaged anomalies over 150–310 m to represent subsurface properties of salinity and temperature.

Significant test

We use the anomaly correlation coefficient (ACC) to evaluate prediction skill. The confidence level of the ACC and the ACC difference is estimated with a block bootstrapping methodology[39]. The 95% confidence interval is the 2.5th and 97.5th percentile range of 1000 random resampling with replacement, and we use block bootstrapping to account for the autocorrelation in the time series. The block length is decided based on the e-folding decorrelation scales in the Nordic Seas, which is 2 years for sea surface salinity (SST) and sea surface salinity (SSS), 3 years for subsurface temperature, and 4 years for subsurface salinity. The two-tailed Student's t test is used to assess the significance of lag correlation and cross-correlation, and the autocorrelation of time series is taken into consideration by calculating the effective degrees of freedom[40].

Index definition

The SPG index in this study is defined as the area-averaged (55–35°W, 50–62°N) density anomaly at 310 m[41], which well captures the connection between the SPG variability and water properties in the eastern subpolar North Atlantic[21]. The SPG strength is positively correlated with the size of the SPG (e.g., Figs. 2d and 4d in Koul et al.[21]) in EN4, also in the MPI-ESM-LR preindustrial control simulation, but less prominent. On average, a strong SPG expands to the eastern SPG region in MPI-ESM-LR. Therefore, the density-based SPG index is well suited to our study. Our findings are robust when we compare against an SPG index defined as the principal component of the second Empirical Orthogonal Function (EOF) of annual mean SSH anomalies[21]. The two SPG indices agree well with each other (Supplementary Fig. 6) and show similar patterns for cross-correlation (Supplementary Fig. 3).

DATA AVAILABILITY

The prediction from the MPI-ESM-LR1.2 decadal prediction system can be accessed via http://hdl.handle.net/hdl:21.14106/098c6104e3d89943248aa61ff69db972adb3baf6[42].

CODE AVAILABILITY

The source codes are available from the corresponding author upon reasonable request.

REFERENCES

1. Borchert, L. F., Müller, W. A. & Baehr, J. Atlantic ocean heat transport influences interannual-to-decadal surface temperature predictability in the North Atlantic region. *J. Clim.* **31**, 6763–6782 (2018).
2. Langehaug, H. R. et al. Propagation of thermohaline anomalies and their predictive potential along the Atlantic water pathway. *J. Clim.* **35**, 2111–2131 (2022).
3. Yeager, S. G. & Robson, J. I. Recent progress in understanding and predicting Atlantic decadal climate variability. *Curr. Clim. Change Rep.* **3**, 112–127 (2017).
4. Langehaug, H. R., Matei, D., Eldevik, T., Lohmann, K. & Gao, Y. On model differences and skill in predicting sea surface temperature in the Nordic and Barents Seas. *Clim. Dyn.* **48**, 913–933 (2017).
5. Borchert, L. F. et al. Improved decadal predictions of North Atlantic subpolar gyre SST in CMIP6. *Geophys. Res. Lett.* **48**, e2020GL091307 (2021).
6. Koul, V. et al. Skilful prediction of cod stocks in the North and Barents Sea a decade in advance. *Commun. Earth Environ.* **2**, 140 (2021).
7. Asbjørnsen, H., Johnson, H. L. & Årthun, M. Variable Nordic Seas inflow linked to shifts in North Atlantic circulation. *J. Clim.* **34**, 7057–7071 (2021).
8. Hátún, H., Sandø, A. B., Drange, H., Hansen, B. & Valdimarsson, H. Influence of the Atlantic subpolar gyre on the thermohaline circulation. *Science* **309**, 1841–1844 (2005).
9. Koul, V., Schrum, C., Düsterhus, A. & Baehr, J. Atlantic inflow to the North Sea modulated by the subpolar gyre in a historical simulation with MPI-ESM. *J. Geophys. Res. Oceans* **124**, 1807–1826 (2019).
10. Sarafanov, A., Falina, A., Sokov, A. & Demidov, A. Intense warming and salinification of intermediate waters of southern origin in the eastern subpolar North Atlantic in the 1990s to mid-2000s. *J. Geophys. Res. Oceans* **113**, C12022 (2008).
11. Årthun, M. & Eldevik, T. On anomalous ocean heat transport toward the Arctic and associated climate predictability. *J. Clim.* **29**, 689–704 (2016).
12. Chepurin, G. A. & Carton, J. A. Subarctic and Arctic sea surface temperature and its relation to ocean heat content 1982-2010. *J. Geophys. Res. Oceans* **117**, C06019 (2012).
13. Holliday, N. P. et al. Reversal of the 1960s to 1990s freshening trend in the northeast North Atlantic and Nordic Seas. *Geophys. Res. Lett.* **35**, L03614 (2008).
14. Koul, V., Brune, S., Baehr, J. & Schrum, C. Impact of decadal trends in the surface climate of the North Atlantic subpolar gyre on the marine environment of the Barents Sea. *Front. Mar. Sci.* **8**, 778335 (2022).
15. Årthun, M. et al. Skillful prediction of northern climate provided by the ocean. *Nat. Commun.* **8**, 15875 (2017).
16. Langehaug, H. R., Sandø, A. B., Årthun, M. & Ilıcak, M. Variability along the Atlantic water pathway in the forced Norwegian Earth System Model. *Clim. Dyn.* **52**, 1211–1230 (2019).
17. Asbjørnsen, H., Årthun, M., Skagseth, Ø. & Eldevik, T. Mechanisms of ocean heat anomalies in the Norwegian Sea. *J. Geophys. Res. Oceans* **124**, 2908–2923 (2019).
18. Mork, K. A. et al. Advective and atmospheric forced changes in heat and fresh water content in the Norwegian Sea, 1951–2010. *Geophys. Res. Lett.* **41**, 6221–6228 (2014).
19. Good, S. A., Martin, M. J. & Rayner, N. A. EN4: Quality controlled ocean temperature and salinity profiles and monthly objective analyses with uncertainty estimates: THE EN4 DATA SET. *J. Geophys. Res. Oceans* **118**, 6704–6716 (2013).
20. Korablev, A., Smirnov, A., Baranova, O. K., Seidov, D. & Parsons, A. R. Climatological Atlas of the Nordic Seas and northern North Atlantic (NCEI Accession 0118478). https://doi.org/10.7289/V54B2Z78 (2014).
21. Koul, V. et al. Unraveling the choice of the north Atlantic subpolar gyre index. *Sci. Rep.* **10**, 1005 (2020).
22. Arthun, M., Wills, R., Johnson, H., Chafik, L. & Langehaug, H. Mechanisms of decadal North Atlantic climate variability and implications for the recent cold anomaly. *J. Clim.* **34**, 3421–3439 (2021).
23. Frankignoul, C. & Hasselmann, K. Stochastic climate models, Part II Application to sea-surface temperature anomalies and thermocline variability. *Tellus* **29**, 289–305 (1977).
24. Burgos, J. M. et al. Predicting the distribution of indicator taxa of vulnerable marine ecosystems in the Arctic and sub-arctic waters of the Nordic Seas. *Front. Mar. Sci.* **7**, 131 (2020).
25. Hegerl, G. C. et al. Toward consistent observational constraints in climate predictions and projections. *Front. Clim.* **3**, 678109 (2021).
26. Giorgetta, M. A. et al. Climate and carbon cycle changes from 1850 to 2100 in MPI-ESM simulations for the Coupled Model Intercomparison Project phase 5: Climate Changes in MPI-ESM. *J. Adv. Model. Earth Syst.* **5**, 572–597 (2013).

27. Mauritsen, T. et al. Developments in the MPI-M Earth System Model Version 1.2 (MPI- ESM1.2) and its response to increasing CO2. *J. Adv. Model. Earth Syst.* **11**, 998–1038 (2019).

28. Brune, S. & Baehr, J. Preserving the coupled atmosphere–ocean feedback in initializations of decadal climate predictions. *WIREs Clim. Change.* **11,** e637 (2020).

29. Hövel, L., Brune, S. & Baehr, J. Decadal prediction of marine heatwaves in MPI-ESM. *Geophys. Res. Lett*. **49**, e2022GL099347 (2022).

30. Polkova, I. et al. Initialization and ensemble generation for decadal climate predictions: a comparison of different methods. *J. Adv. Model. Earth Syst.* **11**, 149–172 (2019).

31. Brune, S., Nerger, L. & Baehr, J. Assimilation of oceanic observations in a global coupled Earth system model with the SEIK filter. *Ocean Model* **96**, 264–264 (2015).

32. Nerger, L. & Hiller, W. Software for ensemble-based data assimilation systems—Implementation strategies and scalability. *Comput. Geosci.* **55**, 110–118 (2013).

33. Wong, A. P. S. et al. Argo Data 1999–2019: two million temperature-salinity profiles and subsurface velocity observations from a global array of profiling floats. *Front. Mar. Sci.* **7**, 00700 (2020).

34. Dee, D. P. et al. The ERA-Interim reanalysis: configuration and performance of the data assimilation system. *Q. J. R. Meteorol. Soc.* **137**, 553–597 (2011).

35. Hersbach, H. et al. The ERA5 global reanalysis. *Q. J. R. Meteorol. Soc.* **146**, 1999–2049 (2020).

36. Uppala, S. M. et al. The ERA-40 re-analysis. *Q. J. R. Meteorol. Soc.* **131**, 2961–3012 (2005).

37. Eyring, V. et al. Overview of the Coupled Model Intercomparison Project Phase 6 (CMIP6) experimental design and organization. *Geosci. Model Dev.* **9**, 1937–1958 (2016).

38. North, G. R., Bell, T. L., Cahalan, R. F. & Moeng, F. J. Sampling errors in the estimation of empirical orthogonal functions. *Mon. Wea. Rev.* **110**, 699–706 (1982).

39. Hans, R. Kunsch. The Jackknife and the bootstrap for general stationary observations. *Ann. Stat.* **17**, 1217–1241 (1989).

40. Bartlett, M. S. Some aspects of the time-correlation problem in regard to tests of significance. *J. R. Stat. Soc.* **98**, 536 (1935).

41. Tesdal, J.-E., Abernathey, R. P., Goes, J. I., Gordon, A. L. & Haine, T. W. N. Salinity trends within the upper layers of the subpolar North Atlantic. *J. Clim.* **31**, 2675–2698 (2018).

42. Brune, S. et al. MPI-ESM-LR_1.2.01p5 decadal predictions localEnKF: monthly mean values. DOKU at DKRZ. http://hdl.handle.net/21.14106/098c6104e3d89943248aa61ff69db972adb3baf6 (2021).

AUTHOR CONTRIBUTIONS

Conception of the work: H.F., L.F.B., and J.B. Acquisition of data: S.B. Analysis and interpretation of data: H.F., L.F.B., S.B., V.K., and J.B. Writing - original draft: H.F. Writing - review & editing: H.F., L.F.B., S.B., V.K., and J.B.

COMPETING INTERESTS

The authors declare no competing interests.

ADDITIONAL INFORMATION

Supplementary information The online version contains supplementary material available at https://doi.org/10.1038/s41612-023-00469-1.

Correspondence and requests for materials should be addressed to Hongdou Fan.

Reprints and permission information is available at http://www.nature.com/reprints

Publisher's note Springer Nature remains neutral with regard to jurisdictional claims in published maps and institutional affiliations.